DOI 10.1007/s11141-016-9636-3
*Radiophysics and Quantum Electronics, Vol. 58, No. 9, February, 2016*
*(Russian Original Vol. 58, No. 9, September, 2015)*

# AUTOMATED MICROWAVE COMPLEX ON THE BASIS OF A CONTINUOUS-WAVE GYROTRON WITH AN OPERATING FREQUENCY OF 263 GHz AND AN OUTPUT POWER OF 1 kW

**M. Yu. Glyavin,[1,2*] M. V. Morozkin,[1] A. I. Tsvetkov,[1] L. V. Lubyako,[1] G. Yu. Golubiatnikov,[1] A. N. Kuftin,[1] V. E. Zapevalov,[1,2] V. V. Kholoptsev,[1] A. G. Eremeev,[1] A. S. Sedov,[1] V. I. Malygin,[1] A. V. Chirkov,[1] A. P. Fokin,[1] E. V. Sokolov,[2] and G. G. Denisov[1,2]**

UDC 621.385.69

*We study experimentally the automated microwave complex for microwave spectroscopy and diagnostics of various media, which was developed at the Institute of Applied Physics of the Russian Academy of Sciences in cooperation with GYCOM Ltd. on the basis of a gyrotron with a frequency of* 263 *GHz and operated at the first gyrofrequency harmonic. In the process of the experiments, a controllable output power of* 0.1–1 *kW was achieved with an efficiency of up to* 17% *in the continuous-wave generation regime. The measured radiation spectrum with a relative width of about* $10^{-6}$ *and the frequency values measured at various parameters of the device are presented. The results of measuring the parameters of the wave beam, which was formed by a built-in quasioptical converter, as well as the data obtained by measuring the heat loss in the cavity and the vacuum output window are analyzed.*

## 1. INTRODUCTION

Many scientific and engineering tasks, such as diagnostics of dense plasma, high-resolution spectroscopy, monitoring of the atmosphere and medical applications, require development of sources of coherent microwave radiation in the frequency range 200–600 GHz with a sufficiently high output power of 0.1–1.0 kW, both in the pulsed and continuous-wave generation regimes. On the one hand, such sources should ensure the parameters of the output radiation, which are required by a specific application, and on the other hand, have a sufficiently high level of automation and control to enable their integration in more complicated systems.

Among the above-mentioned applications, one that is developing most intensely is high-resolution spectroscopy based on nuclear magnetic resonance/dynamic nucleus polarization. Radiation sources for these purposes are developed in the USA (by "CPI–Bruker Biospin"), Japan (by the Research Center for Development of Far-Infrared Region, University of Fukui, FIR FU), Europe, and China. Currently, to produce power levels of tens or hundreds of watts at frequencies exceeding 250 GHz, gyrotrons are used most frequently [1, 2], whose output power exceeds that of the conventional vacuum backward-wave oscillators and semiconductor sources by several orders of magnitude [3], while their cost, size, and operating voltages are significantly lower than those of free-electron lasers [4]. In recent years, a number of gyrotrons producing

* glyavin@appl.sci-nnov.ru

[1] Institute of Applied Physics of the Russian Academy of Sciences; [2] GYCOM Ltd., Nizhny Novgorod, Russia. Translated from Izvestiya Vysshikh Uchebnykh Zavedenii, Radiofizika, Vol. 58, No. 9, pp. 709–719, September 2015. Original article submitted April 24, 2015; accepted September 30, 2015.

0033-8443/16/5809-0639 © 2016 Springer Science+Business Media New York 

radiation in the submillimeter-wave range in the pulsed [5–8] and continuous-wave [9–11] operation regimes have been developed all over the world.

The Institute of Applied Physics of the Russian Academy of Sciences (IAP) and GYCOM Ltd. have jointly developed and manufactured a sealed version of a gyrotron with a built-in quasioptical converter of the operating mode to a narrowly directed wave beam, which ensures generation at a frequency of 263.1 GHz in the continuous-wave regime with a power of up to 1 kW at the fundamental gyrofrequency harmonic, for application in spectroscopy and diagnostics of various media. The device is equipped with a modern automated control system. The results of studying this gyrotron experimentally are presented.

## 2. DESCRIPTION OF THE GYROTRON COMPLEX

It is known that production of strong magnetic fields is a precondition for cyclotron resonance of electrons with the electromagnetic field of the terahertz frequency range. The gyrotron under consideration is installed in a JMTD-10T100 superconducting "dry" cryomagnet (without liquid nitrogen and helium) manufactured by Jastec Inc. (Japan) [12]. The magnet produces a magnetic field of up to 10 T in a warm bore 100 mm in diameter. Such a magnetic system allows one to achieve generation with a frequency of about 263 GHz at the first cyclotron harmonic and also includes an additional magnetic-bias coil, which can be used to adjust parameters of the electron beam and is installed in the cathode region.

The calculated and measured generation frequency of the developed gyrotron is equal to about 263.1 GHz. The calculated value of the output power reached 1 kW in the continuous-wave generation regime at a cathode voltage of 15 kV and an electron beam current of about 0.4 A. Optimization of the electrodynamic system and calculations of the power and efficiency of the device were performed by solving systems of self-consistent equations of the electron–wave interaction using the code developed at IAP. The gyrotron was manufactured by GYCOM Ltd. The emitter of the magnetron-injection gun is made of lanthanum hexaboride $LaB_6$. The electron gun is based on the triode scheme, which in particular allows one to ensure significant flexibility in the process of system adaptation for various applications, e.g., implement fast feedback for stabilization of the output power by varying the anode potential. However, the initial variant for consideration was the use of the gun in the diode regime, with the anode which was short-circuited electrically to the body and had the ground potential. The power of the heater of the thermal cathode in the operating regime is about 80 W, and its power supply was developed and manufactured at IAP. A "Spellman ST20N12X" high-voltage power supply (20 kV and 600 mA) was used as the cathode source, and a "Spellman SL15N1200" power supply (15 kV and 80 mA), as the anode source. The $TE_{5,3}$ mode was chosen as the operating one. The optimal radius $R_b$ of the electron beam in the cavity corresponded to the first maximum in the operating-mode excitation factor. The length of the uniform part in the cavity was chosen to be slightly longer than the optimal one, in order to ensure effective excitation of the operating mode, including the case of a relatively low current of about several tens of milliamperes. Potentially, this allows one to use low-power power supplies for the applications in which the required level of the output power amounts to several tens of watts.

The device is equipped with a built-in quasioptical converter of the operating mode to a narrowly directed wave beam. The converter consists of a waveguide section, a parabolic mirror, and four correcting mirrors. The maximum depth of corrugation on the mirror surfaces is about 0.5 mm at an admissible manufacturing precision of 0.02 mm.

The radiation is output in the horizontal direction through a vacuum window made of boron nitride BN with a diameter of 32 mm and a thickness of 2.7 mm. The exhausted electron beam lands onto the surface of a cone-shaped collector which ensures an acceptable thermal load even in the presence of errors of device adjustment. The gyrotron can operate in both pulsed and continuous-wave generation regimes.

The microwave complex is equipped with an automated control system, which includes original software for user interaction with the gyrotron systems, and other necessary computer equipment. The control system ensures safety of the operator and the complex, acquisition, recording, representation, and logging of information, as well as remote control of various units of the gyrotron system. A block diagram

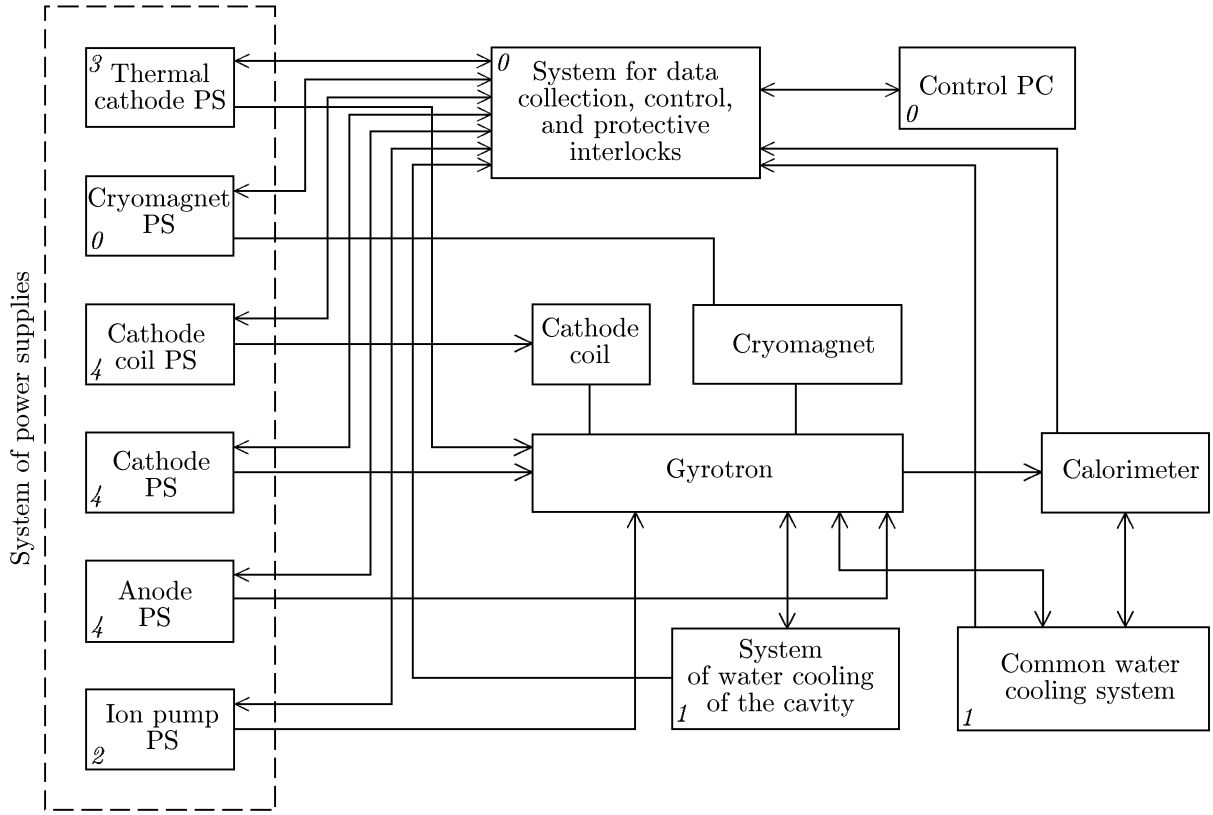


Fig. 1. Block diagram of the microwave complex with a power supply (PS) and a personal computer (PC). In case of failure of one unit of the complex, units with senior numbers are switched off automatically.

of the automated complex is shown in Fig. 1, where the numbers indicate the sequence of switch-on and activation of the protective interlocks of the system. If this or that unit fails, units with senior numbers are deactivated automatically.

This advanced protection system allows a wide circle of researchers (including those without special qualification and skills) to use the complex effectively, which ensures its highly competitive consumer properties.

Figure 2 shows a dialog window of the user software, which displays the current status of each subsystem of the gyrotron complex, represents and enters operating parameters, as well as controls data collection and operating regime of each subsystem.

## 3. CALORIMETRIC MEASUREMENTS OF THE OUTPUT POWER

The output power was measured with a calorimeter installed immediately behind the output window. A block diagram of the measurements is shown in Fig. 3. Two thermal sensors, which measured the water temperatures $t^\circ_{\text{in}}$ and $t^\circ_{\text{out}}$ at the input and output of the calorimeter, respectively, and the heater intended for performing the automated calibration procedure, were installed in the water-cooling contour of the calorimeter. Then the radiated power $P$ was calculated from the temperature difference $t^\circ_{\text{out}} - t^\circ_{\text{in}}$.

We performed a series of calorimetric measurements of the output power as a function of various system parameters. At a power level of 100 W or higher, the error of calorimetric measurements is equal to 10%, and it increases up to 30% at a level of 10 W. The temperature of the water cooling the cavity was maintained at a constant level of 25°C using a special refrigerating machine with an accuracy of 0.5°C. The cryomagnet power supply ("Oxford Instruments Mercury iPS-M") ensures the possibility of adjusting the value of the magnetic field with a step of about $10^{-3}$ T. Figure 4 shows the dependences of the generation power $P$ on the value of the magnetic field $B$ in the cavity, the current $I_{\text{bc}}$ in the bias coil, the electron-beam

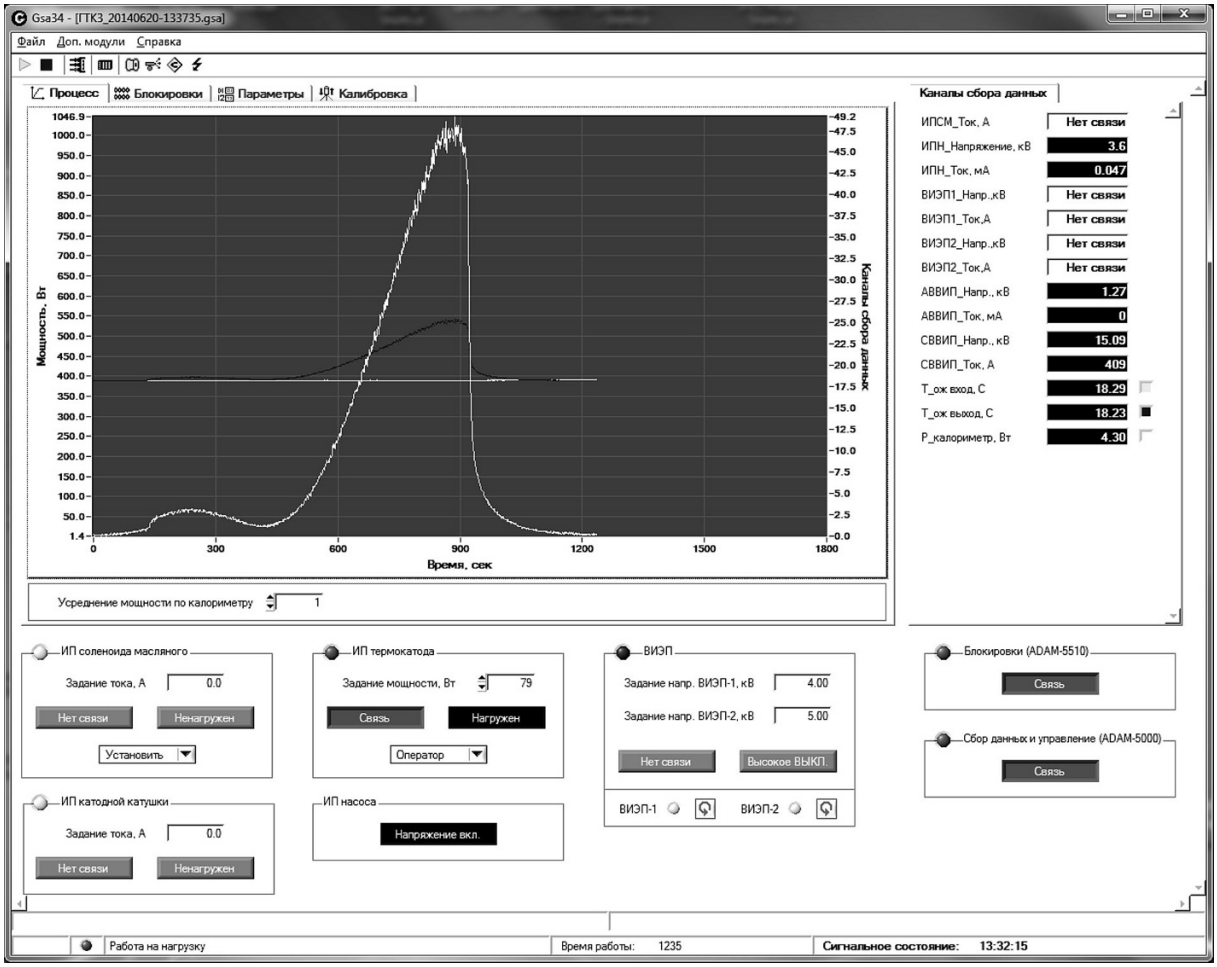


Fig. 2. Dialog window of the application program package for control of the microwave complex.

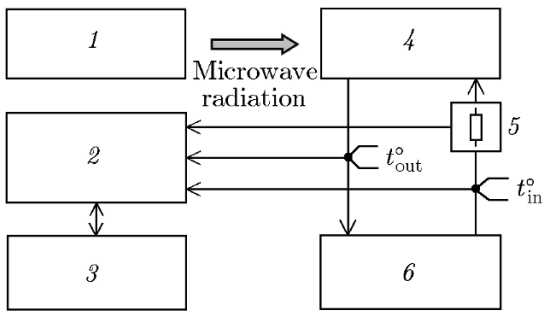


Fig. 3. Block diagram of the calorimetric measurements: gyrotron (*1*), system for data collection, control, and protective interlocks (*2*), controlling PC (*3*), calorimeter (*4*), heater (calibration) (*5*), and common water cooling system (*6*).

current $I$, and the accelerating (cathode) voltage $U$ for the operating $\mathrm{TE}_{5,3}$ mode.

The output power reached more than 0.9 kW at the electron beam current $I = 0.4$ A, a cathode voltage of 15 kV, and a magnetic field of about 9.605 T. In this case, the maximum efficiency amounted to about 17%, which agrees well with the results of the calculations performed at the stage of developing and designing the gyrotron. The output power decreases by approximately two times as the magnetic field increases by 0.4 T. Here, one should bear in mind that the kilowatt level of the generation power is excessive for most spectroscopic applications, where the required power has the order of magnitude of tens of watts. In this connection, the experimentally implemented generation regime at an accelerating voltage of 14 kV and a very low current of 0.02 A seems rather promising. In this regime, a power of about 10 W was achieved with an efficiency of about 3%, which is sufficient for the above-mentioned applications. It should be noted that the possibility of operation in this regime considerably reduces the requirements imposed on the main power supply. At the same time, the regime with a total kilowatt-level power can be necessary for engineering applications.

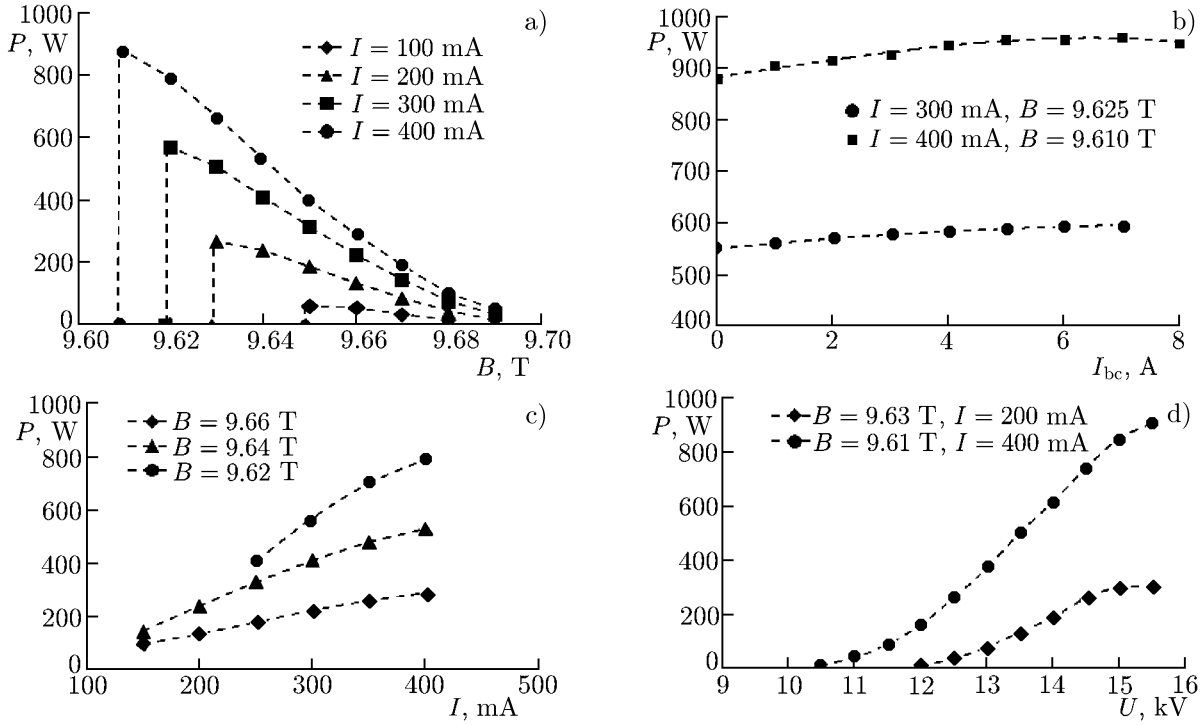


Fig. 4. Dependence of the generation power $P$ on the value of the magnetic field $B$ (*a*), the current $I_{\rm bc}$ in the bias coil (*b*), the electron-beam current $I$ (*c*), and the accelerating voltage $U$ (*d*). In panels *a*–*c*, $U = 15$ kV.

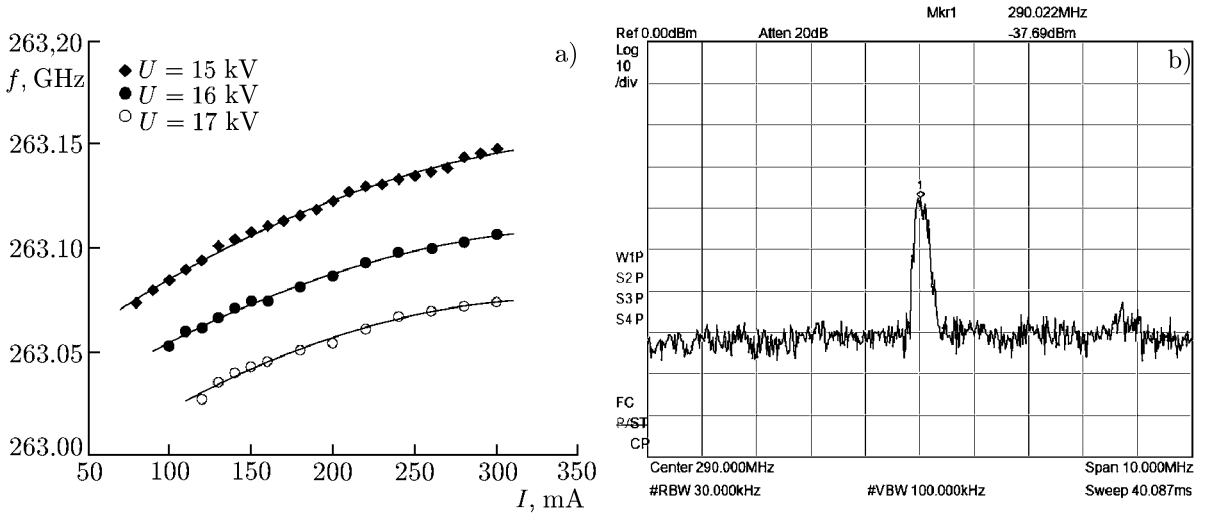


Fig. 5. Generation frequency $f$ as a function of the electron-beam current $I$ for various values of the accelerating voltage $U$ and the cavity temperature $T = 35^\circ$C at $B = 9.67$ T (*a*) and the image of the signal spectrum on the analyzer screen (*b*).

The data obtained show that the choice of the system operation regime in terms of the output power can be made by choosing many parameters. This ensures high flexibility of the system from the viewpoint of its use in various applications. The use of the additional magnetic bias coil, which is installed in the cathode region, allows one to adjust the output radiation parameters in a relatively narrow range, which can be used as a possible mechanism for implementation of the automated power stabilization system.

## 4. MEASUREMENTS OF THE GENERATION FREQUENCY

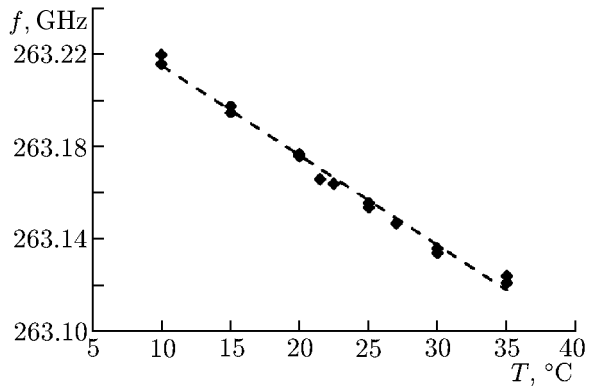


Fig. 6. Generation frequency $f$ as a function of the temperature $T$ of the fluid in the cooling contour of the cavity.

The frequency was measured in the following way. Small part of the radiation was fed to a harmonic mixer through a coupler. In the mixer, it was mixed with a highly stable signal of an external local oscillator having the frequency $f_{\mathrm{LO}}$. The signal from the mixer was sent to the spectrum analyzer at the intermediate frequency $f_{\mathrm{IF}}$. Then, the generation frequency $f$ was determined as $nf_{\mathrm{LO}} \pm f_{\mathrm{IF}}$, where $n$ is the harmonic number. Figure 5*a* shows the experimental dependences of the generation frequency $f$ on the electron beam current $I$ for various values of the accelerating voltage $U$ at the fixed magnetic field $B = 9.67$ T.

The achieved frequency change in the process of temperature variation amounted to about 4 MHz/°C, and in the process of variation of the cathode voltage, to about 33 MHz/kV. The spectrum width $\Delta f$ was equal to about 0.5 MHz ($\Delta f/f \approx 10^{-6}$). Figure 5*b* shows a photo of the display of the spectrum analyzer in the process of the measurements.

Varying the cavity temperature allows one to adjust the device frequency in a relatively narrow range. Figure 6 shows the experimental dependence of the radiation frequency on the temperature of the fluid in the cavity cooling contour at fixed parameters of the device ($B = 9.66$ T, $I = 250$ mA, and $U = 15$ kV).

## 5. THERMAL LOSS IN THE CAVITY AND OUTPUT WINDOW

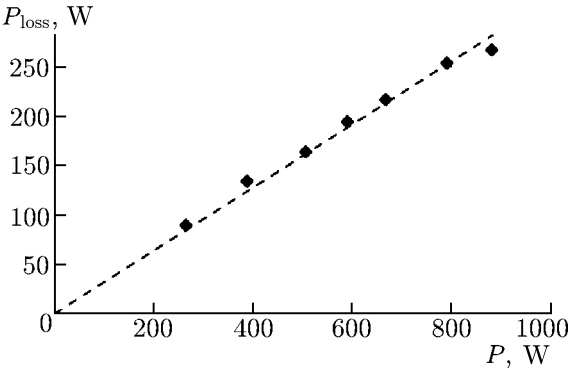


Fig. 7. Dependence of the power of the thermal loss in the cavity walls on the radiated power.

Measuring thermal loss in the cavity and the gyrotron window is extremely important in the context of studying properties of the materials, which they are made of, in the subterahertz frequency range. In particular, it is very important to evaluate the ohmic loss correctly when one chooses the operating regime of low-power terahertz gyrotrons at the development and designing stage. The ohmic Q-factor $Q_{\mathrm{ohm}}$ of the cavity made of ideal copper is usually calculated for the $\mathrm{TE}_{m,p}$ mode by the following formula:

$$Q_{\mathrm{ohm}} = \frac{R_0}{\delta_{\mathrm{skin}}}\left(1 - \frac{m^2}{\nu_{m,p}^2}\right), \qquad (1)$$

where $R_0$ is the radius of the uniform cavity section, $\delta_{\mathrm{skin}}$ is the skin depth, $m$ is the azimuthal index of the mode, and $\nu_{m,p}$ is the mode eigenvalue, which is the $p$th root of the equation $dJ_m(r)/dr = 0$, where $J_m(r)$ is a Bessel function of the first kind. For calculations, a correction factor is usually introduced to this formula. This factor largely depends on the cavity surface roughness, which is determined, in particular, by the manufacturing quality. The ohmic loss value affects the choice of optimal parameters of the gyrotron rather strongly, especially in the case where it becomes comparable with the output power of the device. Therefore, experimental determination of this factor seems dsimportant for refinement of the theoretical model.

The power of the loss in the cavity was performed following the scheme shown in Fig. 3, but the calorimeter cooling contour was switched to the cavity. Figure 7 shows the power of the thermal loss in the cavity walls as a function of the output radiated power.

The ohmic Q-factor was calculated by the relationship $P_{\mathrm{ohm}} = (Q_{\mathrm{dif}}/Q_{\mathrm{ohm}})P$, where $Q_{\mathrm{dif}}$ is the diffraction Q-factor determined at the device designing stage with allowance for the actual geometric sizes

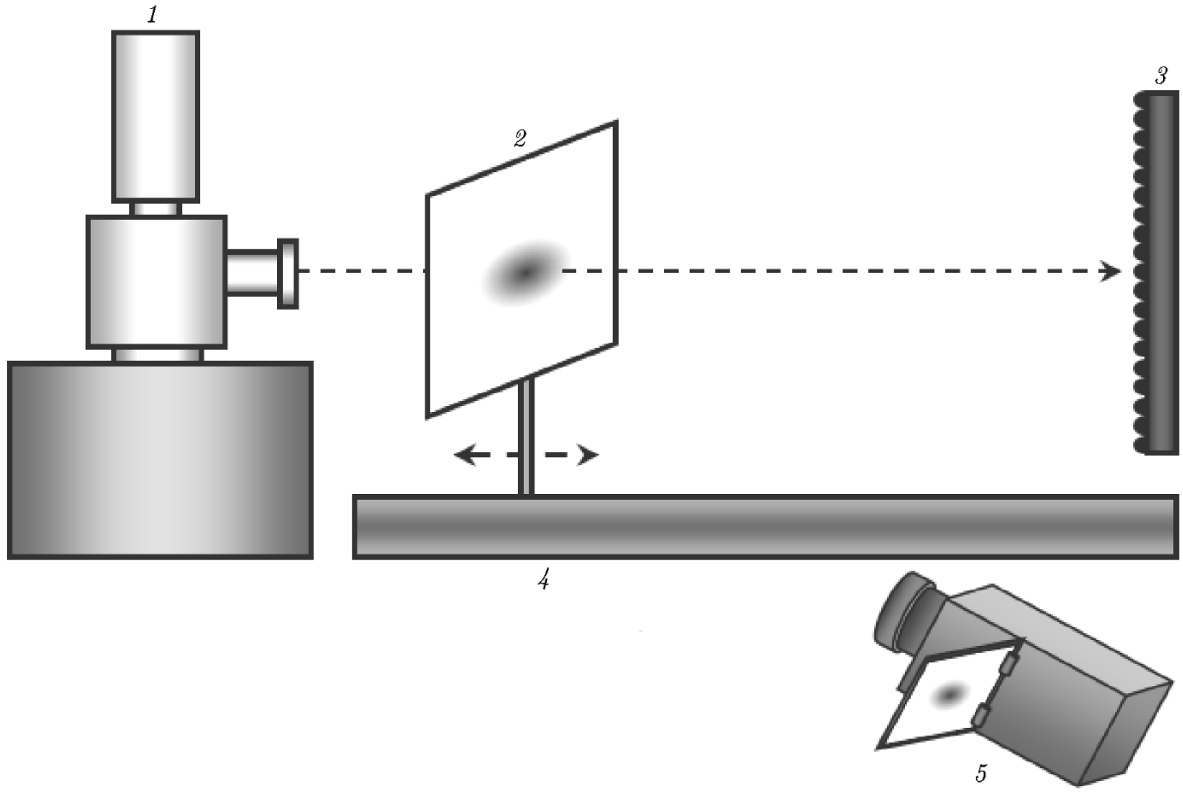


Fig. 8. Scheme of measuring the distribution of the power of the microwave gyrotron radiation using an IR camera: gyrotron (*1*, screen (*2*), load (*3*), guiding rail (*4*), and thermal imager (*5*).

of the cavity. The calculated value of the thermal loss was equal to about 30% of the output radiated power. The calculated value of the ohmic Q-factor $Q_{\text{ohm}}$, which was found by introducing an empirical coefficient of 1/2 to Eq. (1), was equal to about 8800, and the value obtained by the measurements, to about 12000. Thus, the value of the ohmic Q-factor exceeds that of ideal copper by 1.36 times.

The power of the loss in the vacuum window was measured in the same way and amounted to about 7% of the output radiated power, which agrees sufficiently well with the calculated data.

## 6. MEASUREMENT OF THE MICROWAVE POWER DISTRIBUTION IN THE OUTPUT GYROTRON WAVE BEAM

The distribution of the microwave gyrotron power was performed in several cross sections using the IR imaging method, as the wave beam propagated in free space [13]. The measurement scheme is shown in Fig. 8.

A "VarioScan 3021 ST" IR camera, which was used in the measurements, had a high temperature resolution of 0.03°C. This allowed one to obtain a dynamic range no less than 30 dB for the measured data to heat the screen by 30°C. The temperature distribution on the dielectric screen corresponds to the distribution of the intensity of the output microwave gyrotron radiation transmitted through the screen [13]. The measurements were performed in several cross sections, which allowed one to retrieve the phase distribution [14, 15]. In this case, the fact that inverse problems are ill-posed can be controlled using an evident criterion which implies that the obtained solution should obey the wave equation, namely, the transverse amplitude distributions of the reconstructed field should coincide with the measured amplitude distributions in arbitrary cross sections, which are not used in the reconstruction procedure, with accuracy up to experimental errors.

The measured distributions of the field amplitude in the cross sections of the gyrotron wave beam are shown in Fig. 9.

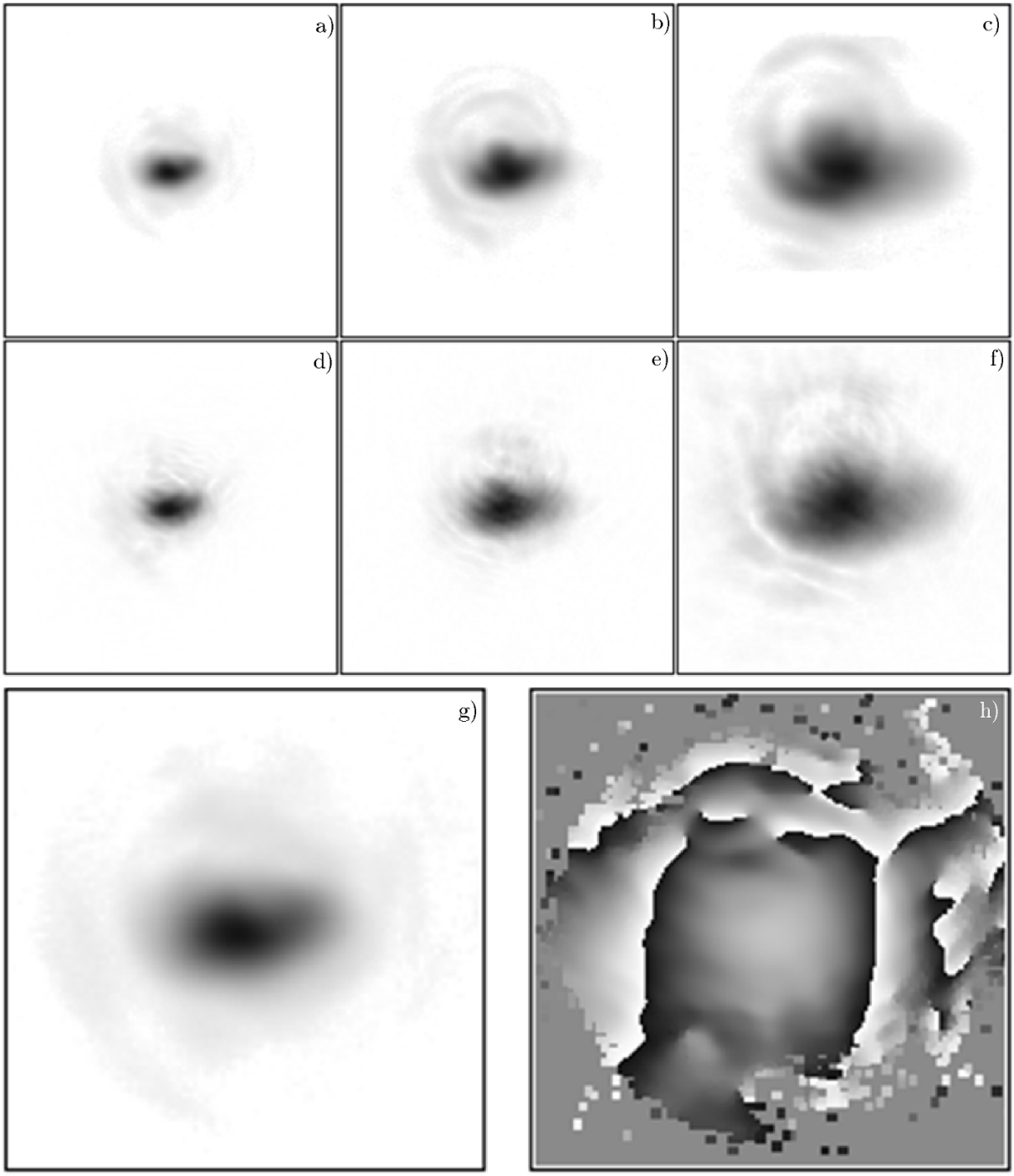


Fig. 9. Measured field distributions in the wave–beam cross sections at different distances from the gyrotron window and the reconstructed distributions of the amplitude in these cross sections. Panels *a* and *d* correspond to a distance of $237$ mm, panels *b* and *e* correspond to $387$ mm, and panels *c* and *f*, to $687$ mm. The aperture is equal to $200 \times 200$ mm. The distributions of the amplitude (*g*) and the retrieved phase (*g*) of the microwave radiation at the distance $Z = 237$ mm from the output window of the gyrotron are also shown. The darker regions correspond to higher values of the amplitude or phase. The $\mathrm{TEM}_{00}$ mode ensures $93\%$ of the measured distribution of the field amplitude.

Figure 9 also shows the retrieved phase distributions in these cross sections, which ensure mutual transformation of the measured amplitude distributions due to diffraction with efficiency values exceeding 98%. Analysis shows that the content of the $TEM_{00}$ mode in the reconstructed wave beam is equal to 93%. Information on the entire three-dimensional structure of the field and first of all that at the input of the mirror system (the two-mirror quasioptical filter), which serves for matching with the transmission line, can be obtained by reconstructing the phase distribution in the cross sections and knowing the amplitude distributions of the wave beam.

## 7. CONCLUSIONS

We have studied the parameters of a continuous-wave gyrotron complex, whose power significantly exceeds that of foreign analogs [9, 10] (a detailed review of the works describing development of terahertz gyrotrons and comparing them with other sources of terahertz radiation are presented, in particular, in [9, 16–18]). Stable single-mode generation at the first gyrofrequency harmonic is achieved, including the case of low operating beam currents, which considerably reduces the requirements imposed on the power and overall dimensions of power supplies. The possibility of frequency tuning by varying the cavity temperature or the operating voltage, which is necessary for many problems, is demonstrated. The fact that the calculated and experimental values of the power, efficiency, and generation frequency correlate well confirms the correctness of the engineering solutions used in the device manufacturing process and allows one to expect successful implementation of microwave systems with frequencies of 527 and 790 GHz, which are to be developed and tested in 2015–2016. The power supplies in such systems will be gyrotrons at the second gyrofrequency harmonic, in which multi-beam electron-optical systems can be applied to improve mode selection.

This work was supported by the Russian Science Foundation (project No. 14–12–00887).

## REFERENCES

1. N. I. Zaytsev, T. B. Pankratova, M. I. Petelin, and V. A. Flyagin, *Radio. Eng. Electron. Phys.*, **19**, 95 (1974).
2. G. S. Nusinovich, *Introduction to the Physics of Gyrotrons*, Johns Hopkins Univ. Press, Baltimore, M.D. (2004), p. 335.
3. J. H. Booske, *Phys. Plasmas*, **15**, No. 5, 055502 (2008).
4. Z. Huang and K.-J. Kim, *Phys. Rev. ST Accel. Beams*, 034801 (2007).
5. T. Idehara, S. Mitsudo, S. Sabchevski, et al., *Vacuum*, **62**, Nos. 2–3, 133 (2001).
6. M. Yu. Glyavin, A. G. Luchinin, and G. Yu. Golubiatnikov, *Phys. Rev. Lett.*, **100**, No. 1, 015101 (2008).
7. V. L. Bratman, Yu. K. Kalynov, and V. N. Manuilov, *Phys. Rev. Lett.*, **102**, No. 24, 245101 (2009).
8. M. Yu. Glyavin, A. G. Luchinin, G. S. Nusinovich, et al., *Appl. Phys. Lett.*, **101**, 153503 (2012).
9. J. H. Booske, R. J. Dobbs, C. D. Joye, et al., *IEEE Trans. Terahertz Sci. Technol.*, No. 1, 54 (2011).
10. T. Idehara and S. P. Sabchevski, *J. Infrared, Millimeter and Terahertz Waves*, **33**, No. 7, 667 (2012).
11. N. P. Venediktov, V. V. Dubrov, V. E. Zapevalov, et al., *Radiophys. Quantum Electron.*, **53**, No. 4, 237 (2010).
12. http://www.jastec-inc.com/e_products_nmr/detail24.html.
13. S. O. Kuznetsov and V. I. Malygin, *Int. J. Infrared Millimeter Waves*, **12**, No. 11, 1241 (1991).
14. A. V. Chirkov, G. G. Denisov, and N. L. Aleksandrov, *Opt. Commun.*, **115**, 449 (1995).
15. A. V. Chirkov and G. G. Denisov, *Int. J. Infrared Millimeter Waves*, **21**, No. 1, 83 (2000).

16. V. Bratman, M. Glyavin, T. Idehara, et al., *IEEE Trans. Plasma Sci.*, **37**, No. 1, 36 (2009).
17. M. Thumm, KIT-SR_7693, KIT Scientific Publishing, Karlsruhe (2014), p. 172.
18. M. Yu. Glyavin, T. Idehara, and S. P. Sabchevski, *IEEE Trans. Terahertz Sci. Technol.*, **5**, No. 5, 788 (2015).